Structural Engineering and Mechanics, Vol. 38, No. 5 (2011) 549-571
DOI: http://dx.doi.org/10.12989/sem.2011.38.5.549

Analytical solutions for skewed thick plates subjected to transverse loading

Pang-jo Chun[1a], Gongkang Fu[2,3,4b] and Yun Mook Lim*[5]

[1]*Department of Civil and Environmental Engineering, Ehime University, Matsuyama, Japan*
[2]*Department of Civil and Environmental Engineering, Wayne State University, Detroit, USA*
[3]*College of Civil Engineering, Tongji University, Shanghai, China*
[4]*College of Civil Engineering, Fuzhou University, Fuzhou, China*
[5]*Department of Civil and Environmental Engineering, Yonsei University, Seoul, Korea*

(Received October 10, 2010, Accepted January 8, 2011)

Abstract. This paper presents analytical solutions for skewed thick plates under transverse loading that have previously been unreported in the literature. The thick plate solution is obtained in a framework of an oblique coordinate system. The governing equation is first derived in the oblique coordinate system, and the solution is obtained using deflection and rotation as partial derivatives of a potential function developed in this research. The solution technique is applied to three illustrative application examples, and the results are compared with numerical solutions in the literature and those derived from the commercial finite element analysis package ANSYS 11. These results are in excellent agreement. The present solution may also be used to model skewed structures such as skewed bridges, to facilitate efficient routine design or evaluation analyses, and to form special elements for finite element analysis. At the same time, the analytical solution developed in this research could be used to develop methods to address post-buckling and dynamic problems.

Keywords: skewed plates; thick plates; Mindlin theory; analytical functions; first order shear deformation theory.

1. Introduction

Skewed plates are important structural elements which are used in a wide range of applications including skewed bridges. In recent decades there have been efforts to analytically investigate the behavior of skewed plates, in spite of the mathematical challenges involved. For example, Morley presented the relationships between rectangular and oblique coordinate systems for load responses in skewed plates (Morley 1962, 1963). This work began with the derivation of a governing equation for isotropic skewed thin plates. The governing equation was analytically solved using a trigonometric series and, numerically, the finite difference method. In deriving the governing equation, the Kirchhoff theory was applied. This assumes that straight lines perpendicular to mid-

*Corresponding author, Associate Professor, E-mail: yunmook@yonsei.ac.kr
[a]Assistant Professor
[b]Professor

surface (i.e., the transverse normals) remain straight and normal to the mid-surface after deformation and the mid-surface does not deform. The Kirchhoff theory is widely used in plate analysis, not only in analytical research (Ramadoss and Nagamani 2009), but also in numerical research including the finite element method (FEM) (Dawe 1966, Monforton and Schmit 1968, Ming and Song 1987, Razaqpur *et al*. 2003), the finite strip method (Tham *et al.* 1986, Wang and Hsu 1994, Cheung and Tham 1998), and the finite difference method (Timoshenko and Woinowsky-Krieger 1959). However, it has the problem of under-predicting deflections when the thickness-to-side ratio becomes large because it neglects the effect of transverse shear deformation (Reddy 2007).

To address this issue, the Mindlin theory was developed by Reissner (1945) and Mindlin (1951). This relaxes the perpendicular restriction for transverse normals and allows them to have an arbitrary but constant rotation to account for the effect of transverse shear deformation. In addition, there are several other theories, such as the ones by Hencky (1947) and Veubeke and Sander (1968).

Several numerical studies on skewed plates have employed the Mindlin theory for static analysis of bending behavior and are worth mentioning. For example, Sengupta (1991, 1995) analyzed isotropic skewed plates using FEM based on the proposed two types of Mindlin triangular plate elements. The paper presented numerical results for different skew angles and support conditions to illustrate the effectiveness of the proposed elements. Ramesh *et al.* (2008, 2009) presented FEM results for the thick plate problem of various shapes with skew using a higher-order triangular plate element based on the Mindlin theory and Reddy's theory. It was concluded that this element can predict stress distribution better than the most commonly used lower-order plate element because stress resultants involve higher-order derivatives of the displacements. Carstensen *et al.* (2010) developed a quadrilateral FEM using the lowest order for Reissner-Mindlin plates on the basis of the Hellinger-Reissner variational principle, which includes variables of displacements, shear stresses and bending moments. Nguyen-Xuan *et al.* (2008) also developed a new type of quadrilateral element with smoothed curvatures for Reissner-Mindlin plates. Their research employed a stabilized conforming nodal integration technique which is used in the mesh-free Galerkin weak form. Due to this characteristic, the element is expected to provide an appropriate answer to the problems of large deformation and strain. Liu *et al.* (2008) and Nguyen-Xuan *et al.* (2010) studied an edge-based smoothed finite element method (ES-FEM) using the 3-node triangular Mindlin element. Compared to conventional FEM, the ES-FEM would offer several advantages, including a higher convergence rate and better computational efficiency. Although the ES-FEM should be able to solve the skewed thick plates problem, their method was only verified by the analytical solution for skewed thin plates because no analytical solution for skewed thick plates was available at that time. The analytical solution developed in our research is expected to give a good benchmark to help such research. Liew and Han (1997) analyzed simply-supported isotropic skewed thick plates using the differential quadrature method (DQM). The DQM approximates a partial derivative of a function at a given discrete point as a weighted linear combination of the function values at all the discrete points. Both thin and thick plates were analyzed under several boundary conditions.

As described above, there are a number of numerical solutions. However, they are quite different to each other and thus it is difficult to judge which of them is valid. Meanwhile, despite these numerical solutions, no analytical or exact solutions have been reported in the literature for skewed thick plates. This paper will report such a solution and is expected to resolve the issue of variation in numerical solutions. First, a governing differential equation based on the Mindlin theory in the oblique coordinate system is developed below, and then it is solved using a sum of polynomial and trigonometric functions. The present method allows consideration of anisotropic materials, various loading conditions, and different boundary conditions.

The governing equation and analytical solution presented in this paper are expected to be further developed in studies including post-buckling analysis and dynamic analysis of skewed thick plates, which have received attention in recent years. For example, Liao and Huang (2008) analyzed post-buckling behavior by the Ritz method, and Garcea (2009) employed FEM to analyze it. Meanwhile, in the vibration analysis, the spline method (Mizusawa and Kondo 2001, Mizusawa *et al.* 2007), the DQM (Liew *et al.* 2003, Malekzadeh 2005, 2008), and the discrete singular convolution method (Gürses *et al.* 2009, Civalek 2009) have been studied. However, although, as shown above, there are a number of numerical solutions, as with the static bending problem, no analytical solution exists at present. Our solution may provide the possibility to develop such an analytical solution.

2. Governing equation in an oblique coordinate system

2.1 Oblique coordinate system

When a plate's boundary profile is a parallelogram, the oblique Cartesian coordinate system can be advantageous. We first present the concept of an oblique coordinate system and then derive the governing differential equation of skewed thick plates based on the Mindlin theory. Fig. 1 shows an oblique coordinate system spanned by the X and Y axes, along with the reference rectangular system by x and y, with angle XOY denoted as skew angle α. Parallelogram $ABCD$ in Fig. 1 represents the skewed plate of interest, and the edge lengths CD and AD are $2a$ and $2b$, respectively.

The relationship between the rectangular and oblique coordinate systems can be written as follows (Morley 1963, Liew and Han 1997, Szilard 2004)

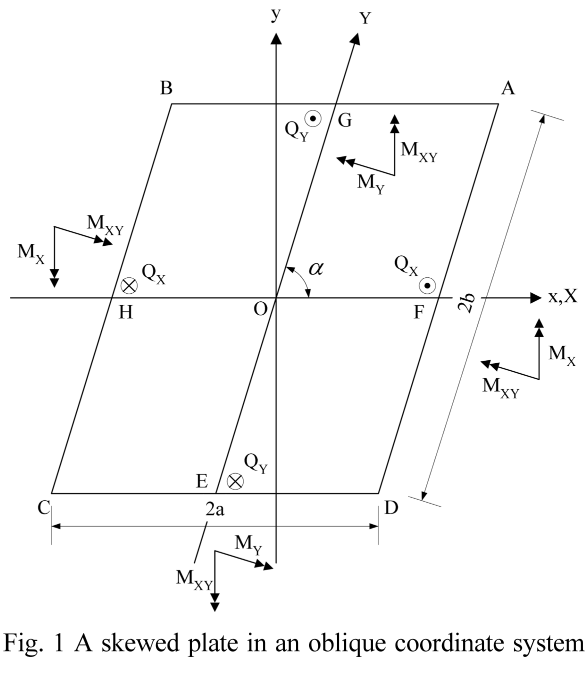

Fig. 1 A skewed plate in an oblique coordinate system

$$\begin{pmatrix} X \\ Y \end{pmatrix} = \begin{pmatrix} 1 & -\cot\alpha \\ 0 & \csc\alpha \end{pmatrix} \begin{pmatrix} x \\ y \end{pmatrix} \tag{1}$$

$$\begin{pmatrix} \dfrac{\partial}{\partial X} \\ \dfrac{\partial}{\partial Y} \end{pmatrix} = \begin{pmatrix} 1 & 0 \\ \cos\alpha & \sin\alpha \end{pmatrix} \begin{pmatrix} \dfrac{\partial}{\partial x} \\ \dfrac{\partial}{\partial y} \end{pmatrix} \tag{2}$$

$$\begin{pmatrix} \phi_X \\ \phi_Y \end{pmatrix} = \begin{pmatrix} 1 & 0 \\ \cos\alpha & \sin\alpha \end{pmatrix} \begin{pmatrix} \phi_x \\ \phi_y \end{pmatrix} \tag{3}$$

where ϕ_X and ϕ_Y are respectively the rotations normal to the X and Y axes. The corresponding relationships for strain, moment, and shear force under the two coordinate systems are also available as follows

$$\begin{pmatrix} \varepsilon_X \\ \varepsilon_Y \\ \gamma_{XY} \end{pmatrix} = \begin{pmatrix} 1 & 0 & 0 \\ \cos^2\alpha & \sin^2\alpha & \sin\alpha\cos\alpha \\ 2\cos\alpha & 0 & \sin\alpha \end{pmatrix} \begin{pmatrix} \varepsilon_x \\ \varepsilon_y \\ \gamma_{xy} \end{pmatrix} \tag{4}$$

$$\begin{pmatrix} M_X \\ M_Y \\ M_{XY} \end{pmatrix} = \begin{pmatrix} \sin\alpha & \cos\alpha\cot\alpha & -2\cos\alpha \\ 0 & \csc\alpha & 0 \\ 0 & -\cot\alpha & 1 \end{pmatrix} \begin{pmatrix} M_x \\ M_y \\ M_{xy} \end{pmatrix} \tag{5}$$

$$\begin{pmatrix} Q_X \\ Q_Y \end{pmatrix} = \begin{pmatrix} \sin\alpha & -\cos\alpha \\ 0 & 1 \end{pmatrix} \begin{pmatrix} Q_x \\ Q_y \end{pmatrix} \tag{6}$$

The moment-strain relationship of the rectangular and oblique coordinate system can be described as in the following Eqs. (7) and (8), respectively (Reddy 2007).

$$\begin{pmatrix} M_x \\ M_y \\ M_{xy} \end{pmatrix} = [D_r] \begin{pmatrix} \varepsilon_x \\ \varepsilon_y \\ \gamma_{xy} \end{pmatrix} \tag{7}$$

$$\begin{pmatrix} M_X \\ M_Y \\ M_{XY} \end{pmatrix} = [D_O] \begin{pmatrix} \varepsilon_X \\ \varepsilon_Y \\ \gamma_{XY} \end{pmatrix} \tag{8}$$

where $[D_r]$ and $[D_o]$ are flexural stiffness matrices of the rectangular and oblique coordinate system. The flexural stiffness matrices relate the moments to the curvatures in the respective coordinate systems. For example, $[D_r]$ in the rectangular coordinate system for isotropic material is (Timoshenko and Woinowsky-Krieger 1959)

$$[D_r] = \frac{Et^3}{12}\begin{pmatrix} \dfrac{1}{1-\nu^2} & \dfrac{\nu}{1-\nu^2} & 0 \\ \dfrac{\nu}{1-\nu^2} & \dfrac{1}{1-\nu^2} & 0 \\ 0 & 0 & \dfrac{1}{2(1+\nu)} \end{pmatrix} \tag{9}$$

where E is Young's modulus, ν is Poisson's ratio, and t is the thickness of the plate.

Since the Mindlin theory assumes that the transverse normals do not experience elongation, Eqs. (7) and (8) are changed into the following Eqs. (10) and (11).

$$\begin{Bmatrix} M_x \\ M_y \\ M_{xy} \end{Bmatrix} = [D_r]\begin{Bmatrix} \dfrac{\partial \phi_x}{\partial x} \\ \dfrac{\partial \phi_y}{\partial y} \\ \dfrac{\partial \phi_x}{\partial y} + \dfrac{\partial \phi_y}{\partial x} \end{Bmatrix} \tag{10}$$

$$\begin{Bmatrix} M_X \\ M_Y \\ M_{XY} \end{Bmatrix} = [D_O]\begin{Bmatrix} \dfrac{\partial \phi_X}{\partial X} \\ \dfrac{\partial \phi_Y}{\partial Y} \\ \dfrac{\partial \phi_X}{\partial Y} + \dfrac{\partial \phi_Y}{\partial X} \end{Bmatrix} \tag{11}$$

From the following calculation (12) based on Eqs. (4), (5), (7), and (8), the flexural stiffness matrix in the oblique coordinate system $[D_o]$ is related to that of the rectangular system $[D_r]$ as in Eq. (13).

$$\begin{aligned}
\begin{pmatrix} M_X \\ M_Y \\ M_{XY} \end{pmatrix} &= \begin{pmatrix} \sin\alpha & \cos\alpha\cot\alpha & -2\cos\alpha \\ 0 & \csc\alpha & 0 \\ 0 & -\cot\alpha & 1 \end{pmatrix}\begin{pmatrix} M_x \\ M_y \\ M_{xy} \end{pmatrix} \\
&= \begin{pmatrix} \sin\alpha & \cos\alpha\cot\alpha & -2\cos\alpha \\ 0 & \csc\alpha & 0 \\ 0 & -\cot\alpha & 1 \end{pmatrix}[D_r]\begin{pmatrix} \varepsilon_x \\ \varepsilon_y \\ \gamma_{xy} \end{pmatrix} \\
&= \begin{pmatrix} \sin\alpha & \cos\alpha\cot\alpha & -2\cos\alpha \\ 0 & \csc\alpha & 0 \\ 0 & -\cot\alpha & 1 \end{pmatrix}[D_r]\begin{pmatrix} 1 & 0 & 0 \\ \cos^2\alpha & \sin^2\alpha & \sin\alpha\cos\alpha \\ 2\cos\alpha & 0 & \sin\alpha \end{pmatrix}^{-1}\begin{pmatrix} \varepsilon_X \\ \varepsilon_Y \\ \gamma_{XY} \end{pmatrix} \\
&= [D_O]\begin{pmatrix} \varepsilon_X \\ \varepsilon_Y \\ \gamma_{XY} \end{pmatrix}
\end{aligned} \tag{12}$$

$$[D_O]=\begin{pmatrix}\sin\alpha & \cos\alpha\cot\alpha & -2\cos\alpha\\ 0 & \csc\alpha & 0\\ 0 & -\cot\alpha & 1\end{pmatrix}[D_r]\begin{pmatrix}1 & 0 & 0\\ \cos^2\alpha & \sin^2\alpha & \sin\alpha\cos\alpha\\ 2\cos\alpha & 0 & \sin\alpha\end{pmatrix}^{-1} \tag{13}$$

Note that Eq. (13) is also applicable for other more complex situations, such as orthotropic or anisotropic materials. In addition, it is pointed out that $[D_o]$ in Eq. (13) is a symmetric matrix when $[D_r]$ is symmetric. The relationships between the shear force and the deflection and rotation angles are described as in Eqs. (14) and (15).

$$\begin{pmatrix}Q_x\\ Q_y\end{pmatrix}=K_s[A_r]\begin{pmatrix}\dfrac{\partial w}{\partial x}+\phi_x\\ \dfrac{\partial w}{\partial y}+\phi_y\end{pmatrix} \tag{14}$$

$$\begin{pmatrix}Q_X\\ Q_Y\end{pmatrix}=K_s[A_O]\begin{pmatrix}\dfrac{\partial w}{\partial X}+\phi_X\\ \dfrac{\partial w}{\partial Y}+\phi_Y\end{pmatrix} \tag{15}$$

where w is the transverse deformation perpendicular to the plane of the plate, K_s is the shear correction factor to account for non-uniform transverse shear distribution, and $[A_r]$ and $[A_o]$ are the extensional stiffness matrices in the rectangular and oblique coordinate system, respectively. The extensional stiffness matrix relates the shear forces to the shear strains. For example, $[A_r]$ for isotropic material is

$$[A_r]=\frac{Et}{2(1+\nu)}\begin{pmatrix}1 & 0\\ 0 & 1\end{pmatrix} \tag{16}$$

From the following calculation (17) based on Eqs. (3), (6), (14), and (15), the extensional stiffness matrix in the oblique coordinate system $[A_o]$ is related to that of the rectangular system $[A_r]$ as in Eq. (18).

$$\begin{aligned}\begin{pmatrix}Q_X\\ Q_Y\end{pmatrix}&=\begin{pmatrix}\sin\alpha & -\cos\alpha\\ 0 & 1\end{pmatrix}\begin{pmatrix}Q_x\\ Q_y\end{pmatrix}\\ &=K_s\begin{pmatrix}\sin\alpha & -\cos\alpha\\ 0 & 1\end{pmatrix}[A_r]\begin{pmatrix}\dfrac{\partial w}{\partial x}+\phi_x\\ \dfrac{\partial w}{\partial y}+\phi_y\end{pmatrix}\\ &=K_s\begin{pmatrix}\sin\alpha & -\cos\alpha\\ 0 & 1\end{pmatrix}[A_r]\begin{pmatrix}1 & 0\\ \cos\alpha & \sin\alpha\end{pmatrix}^{-1}\begin{pmatrix}\dfrac{\partial w}{\partial X}+\phi_X\\ \dfrac{\partial w}{\partial Y}+\phi_Y\end{pmatrix}\end{aligned}$$

$$= K_s[A_O]\begin{pmatrix} \dfrac{\partial w}{\partial X} + \phi_X \\ \dfrac{\partial w}{\partial Y} + \phi_Y \end{pmatrix} \tag{17}$$

$$[A_O] = \begin{pmatrix} \sin\alpha & -\cos\alpha \\ 0 & 1 \end{pmatrix}[A_r]\begin{pmatrix} 1 & 0 \\ \cos\alpha & \sin\alpha \end{pmatrix}^{-1} \tag{18}$$

Similar to the flexural stiffness matrix, $[A_o]$ is a symmetric matrix and also applicable not only for isotropic material, but also other more complex materials. From the relationships derived in this section, the governing equation of skewed thick plate bending is developed in the next section.

2.2 Governing equation of skewed thick plate bending

Hereafter, the components in $[D_o]$ and $[A_o]$ are referred to using their respective elements D_{11} to D_{33} and A_{44} to A_{55} as follows

$$[D_O] = \begin{bmatrix} D_{11} & D_{12} & D_{13} \\ D_{12} & D_{22} & D_{23} \\ D_{13} & D_{23} & D_{33} \end{bmatrix}, [A_O] = \begin{bmatrix} A_{55} & A_{45} \\ A_{45} & A_{44} \end{bmatrix} \tag{19}$$

where the diagonal components of $[D_o]$ relate the moments to the curvatures in the same directions. The off-diagonal terms relate the same moments to the curvatures in other directions due to the Poisson's effect and coordinate system obliquity. Similarly, the diagonal components of $[A_o]$ relate the shear forces to the shear strains in the same directions, and off-diagonal terms to the shear strains in other directions due to obliquity.

The following Eqs. (20) to (22) are equilibrium conditions of the skewed plates shown in Fig. 1.

Equilibrium of force in the z direction

$$\frac{\partial Q_X}{\partial X} + \frac{\partial Q_Y}{\partial Y} = -Q \tag{20}$$

Equilibrium of moments along the X axis

$$\frac{\partial M_Y}{\partial Y} + \frac{\partial M_{XY}}{\partial X} = Q_Y \tag{21}$$

Equilibrium of moments along the Y axis

$$\frac{\partial M_X}{\partial X} + \frac{\partial M_{XY}}{\partial Y} = Q_X \tag{22}$$

where Q in Eq. (20) is the load normal to the upper surface of the plate.

By substituting Eqs. (12), (13), (17) and (18) into (20) to (22), the following Eqs. (23) to (25) are obtained in the oblique system.

$$K_s A_{45}\left(\frac{\partial^2 w}{\partial X \partial Y} + \frac{\partial \phi_X}{\partial Y}\right) + K_s A_{45}\left(\frac{\partial^2 w}{\partial X \partial Y} + \frac{\partial \phi_Y}{\partial X}\right) + K_s A_{55}\left(\frac{\partial^2 w}{\partial X^2} + \frac{\partial \phi_X}{\partial X}\right) + K_s A_{44}\left(\frac{\partial^2 w}{\partial Y^2} + \frac{\partial \phi_Y}{\partial Y}\right) = -Q \tag{23}$$

$$D_{12}\frac{\partial^2\phi_X}{\partial X\partial Y}+D_{13}\frac{\partial^2\phi_X}{\partial X^2}+D_{22}\frac{\partial^2\phi_Y}{\partial Y^2}+D_{23}\left(\frac{\partial^2\phi_X}{\partial Y^2}+2\frac{\partial^2\phi_Y}{\partial X\partial Y}\right)+D_{33}\left(\frac{\partial^2\phi_X}{\partial X\partial Y}+\frac{\partial^2\phi_Y}{\partial X^2}\right)$$
$$=K_sA_{44}\left(\frac{\partial w}{\partial Y}+\phi_Y\right)+K_sA_{45}\left(\frac{\partial w}{\partial X}+\phi_X\right)\tag{24}$$

$$D_{11}\frac{\partial^2\phi_X}{\partial X^2}+D_{12}\frac{\partial^2\phi_Y}{\partial X\partial Y}+D_{13}\left(2\frac{\partial^2\phi_X}{\partial X\partial Y}+\frac{\partial^2\phi_Y}{\partial X^2}\right)+D_{23}\frac{\partial^2\phi_Y}{\partial Y^2}+D_{33}\left(\frac{\partial^2\phi_X}{\partial Y^2}+\frac{\partial^2\phi_Y}{\partial X\partial Y}\right)$$
$$=K_sA_{45}\left(\frac{\partial w}{\partial Y}+\phi_Y\right)+K_sA_{55}\left(\frac{\partial w}{\partial X}+\phi_X\right)\tag{25}$$

To make the solution process simpler, a new function ψ is introduced below to represent the condition of the skewed thick plate. We assume that w consists of terms up to the 4th derivative and ϕ_X and ϕ_Y up to the 3rd derivative of ψ, with respect to the spatial variables X and Y. The following relations in Eqs. (26) to (28) are obtained to satisfy Eqs. (24) and (25).

$$\begin{aligned}w=&(D_{13}^2-D_{11}D_{33})\frac{\partial^4\psi}{\partial X^4}+2(D_{12}D_{13}-D_{11}D_{23})\frac{\partial^4\psi}{\partial X^3\partial Y}+(D_{12}^2-D_{11}D_{22}-2D_{13}D_{23}+2D_{12}D_{33})\frac{\partial^4\psi}{\partial X^2\partial Y^2}+\\&2(-D_{13}D_{22}+D_{12}D_{23})\frac{\partial^4\psi}{\partial X\partial Y^3}+(D_{23}^2-D_{22}D_{33})\frac{\partial^4\psi}{\partial Y^4}+\{A_{44}D_{11}-2A_{45}D_{13}+A_{55}D_{33}\}K_s\frac{\partial^2\psi}{\partial X^2}+\\&2\{A_{44}D_{13}+A_{55}D_{23}-A_{45}(D_{12}+D_{33})\}K_s\frac{\partial^2\psi}{\partial X\partial Y}+\{A_{55}D_{22}-2A_{45}D_{23}+A_{44}D_{33}\}K_s\frac{\partial^2\psi}{\partial Y^2}+(A_{45}^2-A_{44}A_{55})K_s^2\psi\end{aligned}\tag{26}$$

$$\begin{aligned}\phi_X=&(A_{45}D_{13}-A_{55}D_{33})K_s\frac{\partial^3\psi}{\partial X^3}+\{A_{44}D_{13}-2A_{55}D_{23}+A_{45}D_{12}\}K_s\frac{\partial^3\psi}{\partial X^2\partial Y}+\\&\{-A_{55}D_{22}-A_{45}D_{23}+A_{44}(D_{12}+D_{33})\}K_s\frac{\partial^3\psi}{\partial X\partial Y^2}+(-A_{45}D_{22}+A_{44}D_{23})K_s\frac{\partial^3\psi}{\partial Y^3}+(-A_{45}{}^2+A_{44}A_{55})K_s{}^2\frac{\partial\psi}{\partial X}\end{aligned}\tag{27}$$

$$\begin{aligned}\phi_Y=&(-A_{45}D_{11}+A_{55}D_{13})K_s\frac{\partial^3\psi}{\partial X^3}+\{-A_{44}D_{11}-A_{45}D_{13}+A_{55}(D_{12}+D_{33})\}K_s\frac{\partial^3\psi}{\partial X^2\partial Y}+\\&\{-2A_{44}D_{13}+A_{55}D_{23}+A_{45}D_{12}\}K_s\frac{\partial^3\psi}{\partial X\partial Y^2}+(A_{45}D_{23}-A_{44}D_{33})K_s\frac{\partial^3\psi}{\partial Y^3}+(-A_{45}^2+A_{44}A_{55})K_s^2\frac{\partial\psi}{\partial Y}\end{aligned}\tag{28}$$

By substituting these relations into Eq. (23), the governing equation of the Mindlin skewed thick plate is then formulated as a 6th order partial differential equation as follows

$$L(\psi)=-Q\tag{29}$$

where L is a linear differential operator in the oblique coordinate system

$$
\begin{aligned}
L = {} & A_{55}(D_{13}^2 - D_{11}D_{33})K_s \frac{\partial^6}{\partial X^6} + 2\{A_{55}(D_{12}D_{13} - D_{11}D_{23}) + A_{45}(D_{13}^2 - D_{11}D_{33})\}K_s \frac{\partial^6}{\partial X^5 \partial Y} + \\
& \{A_{44}(D_{13}^2 - D_{11}D_{33}) + 4A_{45}(D_{12}D_{13} - D_{11}D_{23}) + A_{55}(D_{12}^2 - D_{11}D_{22} - 2D_{13}D_{23} + 2D_{12}D_{33})\}K_s \frac{\partial^6}{\partial X^4 \partial Y^2} + \\
& \{2A_{44}(D_{12}D_{13} - D_{11}D_{23}) + 2A_{55}(-D_{13}D_{22} + D_{12}D_{23}) + 2A_{45}(D_{12}^2 - 2D_{13}D_{23} + 2D_{12}D_{33} - D_{11}D_{22})\}K_s \frac{\partial^6}{\partial X^3 \partial Y^3} + \\
& \{A_{44}(D_{12}^2 - D_{11}D_{22} - 2D_{13}D_{23} + 2D_{12}D_{33}) + A_{55}(D_{23}^2 - D_{22}D_{33}) + 4A_{45}(D_{12}D_{23} - D_{13}D_{22})\}K_s \frac{\partial^6}{\partial X^2 \partial Y^4} + \\
& 2\{A_{45}(D_{23}^2 - D_{22}D_{33}) + A_{44}(D_{12}D_{23} - D_{13}D_{22})\}K_s \frac{\partial^6}{\partial X \partial Y^5} + A_{44}(D_{23}^2 - D_{22}D_{33})K_s \frac{\partial^6}{\partial Y^6} + \\
& D_{11}(A_{44}A_{55} - A_{45}^2)K_s^2 \frac{\partial^4}{\partial X^4} + 4D_{13}(A_{44}A_{55} - {A_{45}}^2)K_s^2 \frac{\partial^4}{\partial X^3 \partial Y} + 2(D_{12} + 2D_{33})(A_{44}A_{55} - {A_{45}}^2)K_s^2 \frac{\partial^4}{\partial X^2 \partial Y^2} + \\
& 4D_{23}(A_{44}A_{55} - A_{45}^2)K_s^2 \frac{\partial^4}{\partial X \partial Y^3} + D_{22}(A_{44}A_{55} - A_{45}^2)K_s^2 \frac{\partial^4}{\partial Y^4}
\end{aligned} \tag{30}
$$

3. Analytical solution in series form

In this section, a general solution to the governing differential equation Eq. (29) is developed as the sum of a fundamental (homogeneous) and a particular (non-homogeneous) solution, detailed separately next.

3.1 Homogeneous solution

The homogeneous solution $\o_h$ is the solution to Eq. (29) for Q = 0, obtained as a sum of polynomials ψ_{hp} in Eq. (31) and trigonometric series ψ_{ht} in Eq. (32) below.

$$
\begin{aligned}
\psi_{hp} = {} & Z_1 + Z_2X + Z_3Y + Z_4X^2 + Z_5Y^2 + Z_6XY + Z_7X^3 + Z_8X^2Y + Z_9XY^2 + Z_{10}Y^3 + \\
& Z_{11}(D_{22}(-{A_{45}}^2 + A_{44}A_{55})X^4 - D_{11}(-{A_{45}}^2 + A_{44}A_{55})Y^4) + Z_{12}(D_{23}(-{A_{45}}^2 + A_{44}A_{55})X^3Y - D_{13}(-{A_{45}}^2 + A_{44}A_{55})XY^3)
\end{aligned} \tag{31}
$$

$$
\begin{aligned}
\psi_{ht} = \sum_{h=1}^{\infty} (& A_hC_{1X1} + iB_hC_{1X2} + C_hC_{2X1} + iD_hC_{2X2} + E_hC_{3X1} + iF_hC_{3X2} + G_hS_{1X1} + iH_hS_{1X2} + I_hS_{2X1} + \\
& iJ_hS_{2X2} + K_hS_{3X1} + iL_hS_{3X2} + M_hC_{1Y1} + iN_hC_{1Y2} + O_hC_{2Y1} + iP_hC_{2Y2} + Q_hC_{3Y1} + iR_hC_{3Y2} + \\
& S_hS_{1Y1} + iT_hS_{1Y2} + U_hS_{2Y1} + iV_hS_{2Y2} + W_hS_{3Y1} + iX_hS_{3Y2})
\end{aligned} \tag{32}
$$

Where $i = \sqrt{-1}$ is the imaginary unit, and C_{eXf}, C_{eYf}, S_{eXf}, and S_{eYf} are trigonometric functions as follows

$$C_{eXf} = \cos\frac{\pi h(X+\lambda_{eY}Y)}{2a} + (-1)^{f+1}\cos\frac{\pi h(X+\bar{\lambda}_{eY}Y)}{2a}$$
$$S_{eXf} = \sin\frac{\pi h(X+\lambda_{eY}Y)}{2a} + (-1)^{f+1}\sin\frac{\pi h(X+\bar{\lambda}_{eY}Y)}{2a}$$
$$C_{eYf} = \cos\frac{\pi h(\lambda_{eX}X+Y)}{2b} + (-1)^{f+1}\cos\frac{\pi h(\bar{\lambda}_{eX}X+Y)}{2b}$$
$$S_{eYf} = \sin\frac{\pi h(\lambda_{eX}X+Y)}{2b} + (-1)^{f+1}\sin\frac{\pi h(\bar{\lambda}_{eX}X+Y)}{2b} \tag{33}$$
$$(e = 1,2,3,\ f = 1,2)$$

where the bar on λ denotes the conjugate of λ. λ_{1X}, λ_{2X}, λ_{3X}, λ_{1Y}, λ_{2Y}, and λ_{3Y} are the eigenvalues to be obtained by satisfying $L(\psi_{ht}) = 0$. For example, λ_{eX} is derived by solving the following equation.

$$L\left(\cos\frac{\pi h(\lambda_{eX}X+Y)}{2a} + \sin\frac{\pi h(\lambda_{eX}X+Y)}{2a}\right) = 0 \tag{34}$$

The polynomial function ψ_{hp} in Eq. (31) has 12 unknowns Z_1 to Z_{12}, and the trigonometric function ψ_{ht} in Eq. (32) has 24l unknowns A_h, B_h, Ch, …, and X_h (h = 1, 2, 3,…, l) with l being the number of the trigonometric terms needed for convergence. Therefore, the homogeneous solution ψ_h has 24l+12 unknowns and they will be determined according to the boundary conditions discussed below.

3.2 Particular solution

For a particular solution in the series form, the transverse load Q in Eq. (29) is expanded to a trigonometric series as in the following Eqs. (35) and (36) to express a uniform distributed load and a concentrated load, respectively.

$$Q = \sum_{j=1,3,\ldots}^{\infty}\sum_{k=1,3,\ldots}^{\infty} \frac{16q_0(-1)^{(j+k+2)/2}}{jk\pi^2}\cos\frac{j\pi X}{2a}\cos\frac{k\pi Y}{2b}\sin\alpha \tag{35}$$

$$Q = \frac{Q_0}{ab}\sum_{j=1,2,\ldots}^{\infty}\sum_{k=1,2,\ldots}^{\infty} \sin\frac{j\pi(X_0+a)}{2a}\sin\frac{j\pi(X+a)}{2a}\sin\frac{k\pi(Y_0+b)}{2b}\sin\frac{k\pi(Y+b)}{2b} \tag{36}$$

where q_0 is the uniformly distributed load, Q_0 is the concentrated load at point (X_0, Y_0). Parenthetically, we note that not only the uniform distributed load and the concentrated load, but also a line load and patch load can be expressed as trigonometric series. The solution of inhomogeneous Eq. (29) is described as ψ_p and it can be derived as the following Eqs. (37) and (38) when Q is given as Eqs. (35) and (36), respectively.

$$\psi_p = \sum_{j=1,3,\ldots}^{m}\sum_{k=1,3,\ldots}^{m}\left(K_{jk}\cos\frac{j\pi X}{2a}\cos\frac{k\pi Y}{2b} + L_{jk}\sin\frac{j\pi X}{2a}\sin\frac{k\pi Y}{2b}\right) \tag{37}$$

$$\psi_b = \sum_{j=1,2,\ldots}^{m}\sum_{k=1,2,\ldots}^{m} K_{jk}\cos\frac{j\pi(X+a)}{2a}\cos\frac{k\pi(Y+b)}{2b} + L_{jk}\sin\frac{j\pi(X+a)}{2a}\sin\frac{k\pi(Y+b)}{2b} \tag{38}$$

where K_{jk} and L_{jk} are to be determined to satisfy Eq. (29) for all X and Y, m is the number of the trigonometric terms needed for convergence. The general solution for ψ is derived as the sum of the homogeneous solution and the particular solution as

$$\psi = (\psi_{hp} + \psi_{ht}) + \psi_p \tag{39}$$

Since no unknowns exist in the particular solution, the total number of unknowns in the general solution is still $24l$+12, as in the homogeneous solution.

4. Determination of unknown constants for series solution

In the Mindlin theory, the boundary conditions for various edges are given below for determining the unknown constants in the homogeneous solution. The normal and tangential directions to the edge are denoted here using subscripts n and s respectively. The moments on the edges are accordingly noted using these subscripts consistent with the directions of the stresses thereby induced. Namely M_n is for the moment causing normal stresses and M_s is the torsional moment inducing shear stresses.

(1) Clamped: $w = \overline{w}, \phi_n = \overline{\phi}_n, \phi_s = \overline{\phi}_s$ (40)

(2) Soft Simply Supported (SS1) : $w = \overline{w}, M_n = \overline{M}_n, \phi_s = \overline{\phi}_s$ (41)

(3) Hard Simply Supported (SS2): $w = w, M_n = \overline{M}_n, M_s = \overline{M}_s$ (42)

(4) Free: $M_n = \overline{M}_n, M_s = \overline{M}_s, Q_n = \overline{Q}_n$ (43)

Here, w, ϕ_n, ϕ_s with the bar indicate the enforced displacement, and M_n, M_s, Q_n with the bar

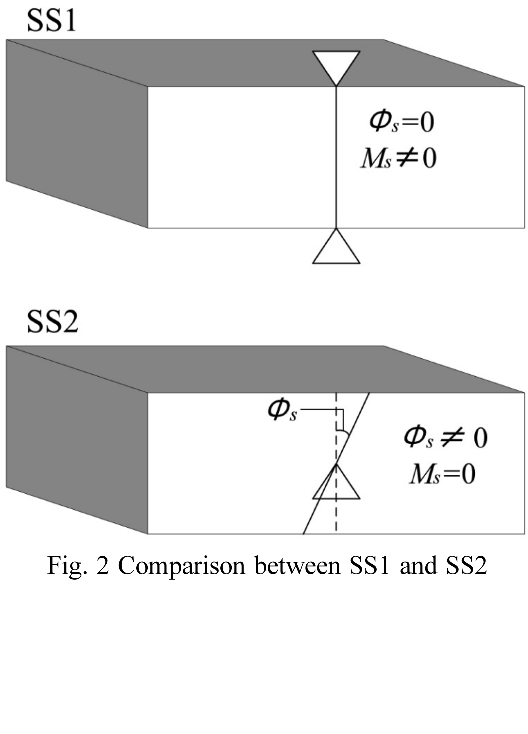

Fig. 2 Comparison between SS1 and SS2

indicate the external force along the edge. Note that the Kirchhoff theory treats SS1 and SS2 in Eqs. (41) and (42) as the same boundary condition. The difference between them is explained graphically in Fig. 2 when the variables with bar are zero (Hangai 1995). The boundary condition of SS1 restricts the tangential rotation by supporting two points in the cross section, thereby generating a non-zero torsional moment. In contrast, the boundary condition of SS2 supports the plate only at one point in the cross section, allowing a tangential rotation and generating no twisting moment.

The boundary conditions in Eqs. (40) to (43) can be unified as follows

$$\Gamma_d(X,Y)=\bar{\Gamma}_d(X,Y)\begin{cases} d=1,2,3 & (\text{edge } CD \text{ in Fig. 1}) \\ d=4,5,6 & (\text{edge } AB \text{ in Fig. 1}) \\ d=7,8,9 & (\text{edge } BC \text{ in Fig. 1}) \\ d=10,11,12 & (\text{edge } AD \text{ in Fig. 1}) \end{cases} \tag{44}$$

where $\Gamma_1(X, Y)$ to $\Gamma_{12}(X, Y)$ represent the left hand side of Eqs. (40) to (43) and the meaning of the bar is the same. $\Gamma_1(X, Y)$ to $\Gamma_{12}(X, Y)$ are expanded as a Fourier series as follows for the solution method pursued in this paper

$$\Gamma_d(X,Y)=\frac{a_{0d}}{2}+\sum_{c=1}^{\infty}\left(a_{cd}\cos\left(\frac{c\pi X}{a}\right)+b_{cd}\sin\left(\frac{c\pi X}{a}\right)\right)\ (d=1,2,\ldots,6)\ \ (\text{for the edge of } Y=b,\,-b)$$

$$\Gamma_d(X,Y)=\frac{a_{0d}}{2}+\sum_{c=1}^{\infty}\left(a_{cd}\cos\left(\frac{c\pi Y}{b}\right)+b_{cd}\sin\left(\frac{c\pi Y}{b}\right)\right)\ (d=7,8,\ldots,12)\ \ (\text{for the edge of } X=a,\,-a) \tag{45}$$

where coefficients a_{0d}, a_{cd}, and b_{cd} are Fourier coefficients for boundary condition $\Gamma_d(X, Y)$. In the same manner, $\Gamma_d(X, Y)$ with the bar are also expanded. For necessary truncation, l terms are kept for each of the 12 boundary conditions so that a total of $12(2l+1)$ equations are to be established as in Eq. (46).

$$\begin{cases} a_{0d}=\bar{a}_{0d} \\ a_{cd}=\bar{a}_{cd} \\ b_{cd}=\bar{b}_{cd} \end{cases} \quad (c=1,\ldots,l,\ d=1,\ldots,12) \tag{46}$$

where the variable with bar is the fourier coefficients of $\Gamma_d(X, Y)$ with the bar. The simultaneous Eq. (46) include the $24l+12$ unknowns and can be solved because the number of equations and unknowns are the same.

5. Application examples

In this section, three application examples are presented using the developed analytical method for skewed thick plates. They are also compared with solutions published in the literature, and with the FEM analysis result obtained using a commercial package ANSYS 11. In the analysis by ANSYS, 2D 4-node quadrilateral plate elements (SHELL181) appropriate for thick plate analysis are used for the skewed plates with various skewed angles. For skewed plates of which the skewed angle $\alpha = 30°$, 45°, 60°, 75°, and 90° the numbers of nodes and elements are 1683 and 1523, respectively. In contrast, for skewed angle $\alpha = 15°$, 2 triangular elements are used at acute corners to avoid an extensively skewed element. Consequently, the numbers of nodes and elements are 1650 and 1493, respectively. In addition, the effect on convergence of the number of terms l and m in the fundamental and particular solutions is studied. In the following examples, the shear correction factor K_s is taken as 5/6, as is commonly used in plate analyses.

5.1 Simply supported isotropic skewed thin plate under uniformly distributed load

Isotropic thin skewed plates are analyzed here. As an external force, uniformly distributed load q_0 is applied and as skewed angles, $\alpha = 15°$, 30°, 45°, 60°, 75°, and 90° are employed. The geometrical properties used in this research are $a = b$, and $t = 0.02\ a$. The SS2 boundary condition in Eq. (42) is used for all edges.

As a first step, the numbers of terms in the series solution l and m are determined. Fig. 3 shows the out-of-plane deflection w at the center of the $a = 30°$ plate against the numbers of terms l and m in Eq. (37). Also the expansion of the transverse load Q and the boundary conditions Γ_d used respectively m and l terms. To see the trend of convergence as a function of l, Fig. 3 shows the results of increasing the number of terms m, for four different l values. The vertical axis shows the deflection normalized by that of $l = 7$ and $m = 55$, denoted as $(l, m) = (7, 55)$. As seen, the deflection w for (l, m)=(5, 55) and (7, 35) differs by less than 0.5% from that of (l, m)=(7, 55). It can be concluded that the solution is already convergent while truncated at (l, m)=(7, 55) and therefore $l = 7$ and $m = 55$ are employed in this example. Note that for different skew angles, similar results are observed.

Table 1 is a comparison between the present and the previous results of the deflection w_c, maximum principal moment $M_{\max c}$, and minimum principal moment $M_{\min c}$ at the center of the plate $(X, Y) = (0, 0)$. The deflection and moment are expressed in a dimensionless form as $100 w_c D/q_0 a^4$

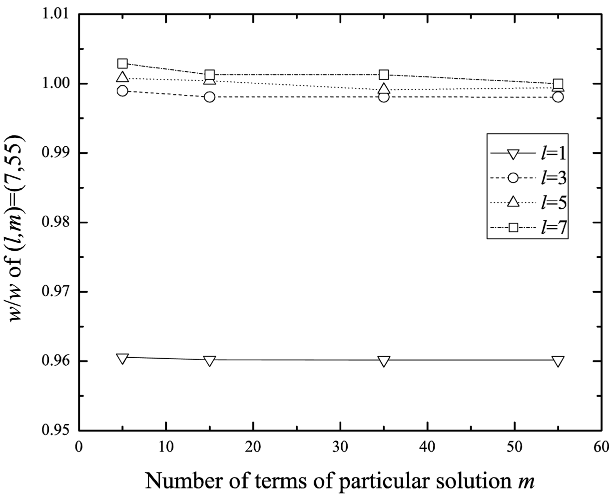

Fig. 3 Truncation effect for convergence for center deflection of simply supported (SS2) isotropic 30 degrees skewed thin plate under uniform loading

Table 1 Deflection, maximum moment, and minimum moment at the center of simply supported (SS2) skewed thin plates under uniform loading (value in parentheses is error ratio)

α		$100w_cD/q_0a^4$	$10M_{\max c}/q_0a^2$	$10M_{\min c}/q_0a^2$
75°	Present Study	5.8513	1.9318	1.7191
	ANSYS	5.8662 (0.25%)	1.9215 (-0.53%)	1.7074 (-0.68%)
	Butalia *et al*. (1990)	5.8013 (-0.85%)	1.9207 (-0.57%)	1.7082 (-0.63%)
	GangaRao and Chaudhary (1998)	5.8240 (-0.47%)	N/A	N/A
	Liew and Han (1997)	5.9257 (1.27%)	1.9512 (1.00%)	1.7261 (0.41%)
	Sengupta (1991)	5.8468 (-0.77%)	1.9241 (-0.40%)	1.7097 (-0.55%)
	Sengupta (1995)	5.8172 (-0.58%)	1.9030 (1.49%)	1.6931 (-1.51%)
60°	Present Study	4.1946	1.7227	1.3614
	ANSYS	4.1455 (-1.17%)	1.7051 (-1.02%)	1.3372 (-1.78%)
	Butalia *et al*. (1990)	3.9832 (-5.04%)	1.6790 (-2.54%)	1.2980 (-4.66%)
	GangaRao and Chaudhary (1998)	4.0960 (-2.35%)	N/A	N/A
	Liew and Han (1997)	4.1908 (-0.09%)	1.7349 (0.71%)	1.3561 (-0.39%)
	Morley (1963)	4.0960 (-2.35%)	1.7000 (-1.32%)	1.3320 (-2.16%)
	Muhammad and Singh (2004)	4.0960 (-2.35%)	1.7240 (0.08%)	1.3720 (0.78%)
	Sengupta (1991)	4.1123 (-1.96%)	1.7075 (-0.88%)	1.3391 (-1.64%)
	Sengupta (1995)	4.1079 (-2.07%)	1.6909 (-1.85%)	1.3267 (-2.54%)
45°	Present Study	2.2105	1.3289	0.9075
	ANSYS	2.1498 (-2.75%)	1.2955 (-2.51%)	0.8824 (-2.76%)
	Argyris (1965)	2.0787 (-5.96%)	1.2983 (-2.30%)	0.8570 (-5.56%)
	Butalia *et al*. (1990)	1.9125 (-13.5%)	1.2266 (-7.70%)	0.7803 (-14.0%)
	GangaRao and Chaudhary (1998)	2.1120 (-4.46%)	N/A	N/A
	Liew and Han (1997)	2.1669 (-1.97%)	1.3194 (-0.71%)	0.9032 (-0.47%)
	Sengupta (1991)	2.1330 (-3.51%)	1.2995 (-2.21%)	0.8866 (-2.30%)
	Sengupta (1995)	2.1285 (-3.71%)	1.2892 (-2.99%)	0.8787 (-3.17%)
30°	Present Study	0.6824	0.7888	0.4678
	ANSYS	0.6721 (-1.51%)	0.7656 (-2.94%)	0.4482 (-4.19%)
	Argyris (1965)	0.6158 (-9.76%)	0.7668 (-2.79%)	0.4028 (-13.9%)
	Butalia *et al*. (1990)	0.5194 (-23.9%)	0.6662 (-15.5%)	0.3166 (-32.3%)
	Carstensen *et al*. (2010)	0.6784 (-0.59%)	N/A	N/A
	GangaRao and Chaudhary (1998)	0.6496 (-4.81%)	N/A	N/A
	Jirousek (1987)	0.6526 (-4.37%)	0.7625 (-3.33%)	0.4343 (-7.16%)
	Liew and Han (1997)	0.6679 (-2.12%)	0.7780 (-1.37%)	0.4509 (-3.61%)
	Morley (1963)	0.6528 (-4.34%)	0.7640 (-3.14%)	0.4320 (-7.65%)
	Muhammad and Singh (2004)	0.5658 (-17.1%)	0.6800 (-13.8%)	0.3405 (-27.2%)
	Razaqpur *et al*. (2003)	0.6771 (-0.78%)	0.7568 (-4.06%)	0.4441 (-5.07%)
	Sengupta (1991)	0.6690 (-1.97%)	0.7734 (-1.95%)	0.4481 (-4.21%)
	Sengupta (1995)	0.6587 (-3.47%)	0.7628 (-3.30%)	0.4340 (-7.23%)
15°	Present Study	0.0658	0.2637	0.1220
	ANSYS	0.0650 (-1.22%)	0.2580 (-2.17%)	0.1194 (-2.13%)
	Butalia *et al*. (1990)	0.0422 (-35.9%)	0.1906 (-27.7%)	0.0639 (-47.6%)
	Liew and Han (1997)	0.0635 (-3.50%)	0.2566 (-2.69%)	0.1149 (-5.82%)
	Sengupta (1991)	0.0653 (-0.76%)	0.2586 (-1.93%)	0.1226 (0.49%)
	Sengupta (1995)	0.0605 (-8.05%)	0.2461 (-6.67%)	0.1030 (-15.6%)

and $10M_c/q_0a^2$, where w_c and M_c are the deflection and moment at the center of the plate, and D is the bending stiffness and is expressed as $D = Et^3/12(1-\nu^2)$.

In the case of $\alpha = 15°$, 30°, a significant difference is observed between the present solution and the solution of Butalia *et al.* (1990). The latter indicated in their literature that the result by their method is not necessarily correct when α is less than 45° and the present analysis bears this out. In addition, in the case of $\alpha = 30°$, the results of Muhammad and Singh (2004) shows significant difference with the present results. They also have recognized this problem, and mentioned that the problem is resolved when the boundary is clamped. It has been felt that their shape function fails to estimate the simply supported condition along the skew edge which requires evaluating the moment and torsion precisely. Furthermore, in the case of $\alpha = 15°$, the results of Sengupta (1991) and Sengupta (1995) are different. The present result indicates that the result of Sengupta (1991) is closer to the exact solution. For other cases, the present result is in good agreement with the previous result and the finite element analysis result.

Figs. 4 to 7 are the comparison between the present method and FEM analysis using ANSYS for the deflection w and strains ε_x, ε_y, and ε_{xy} defined in the following Eq. (47) for $\alpha = 30°$, 60°, and 90° along line HF defined in Fig. 1 and on the top of the plate.

$$\begin{Bmatrix} \varepsilon_x \\ \varepsilon_y \\ \varepsilon_{xy} \end{Bmatrix} = \frac{t}{2}\begin{Bmatrix} \dfrac{\partial \phi_x}{\partial x} \\ \dfrac{\partial \phi_y}{\partial y} \\ \dfrac{\partial \phi_x}{\partial y} + \dfrac{\partial \phi_y}{\partial x} \end{Bmatrix} \tag{47}$$

The deflection and strains are normalized as $100wD/q_0a^4$ and $100D\varepsilon/q_0a^2t$. The results show that our analytical and the numerical solutions agree with each other very well for these isotropic thin skewed plates under the uniformly distributed load. The deflection w in Fig. 4 is shown to decrease

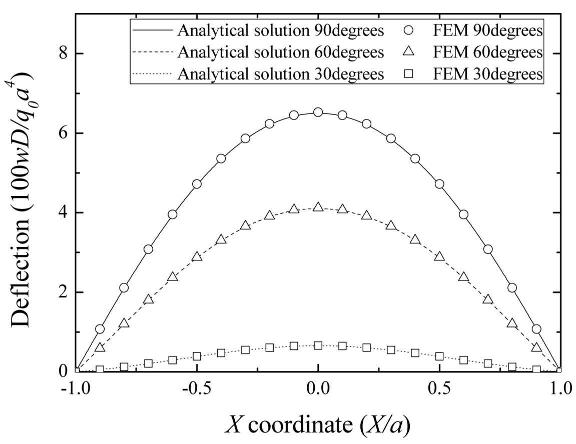

Fig. 4 Analytical and FEM solutions for deflection of simply supported (SS2) isotropic skewed thin plate under uniform loading

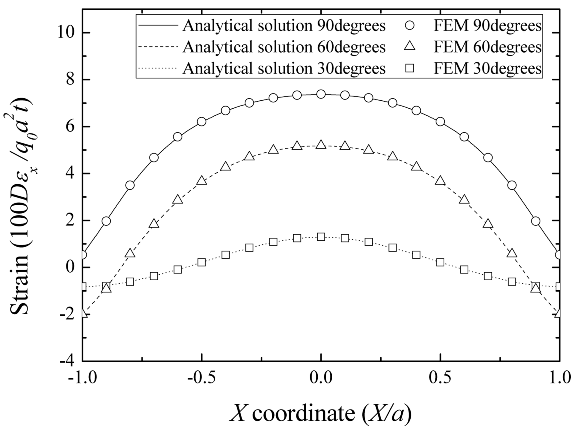

Fig. 5 Analytical and FEM results of x-direction strain of simply supported (SS2) isotropic skewed thin plate under uniform loading

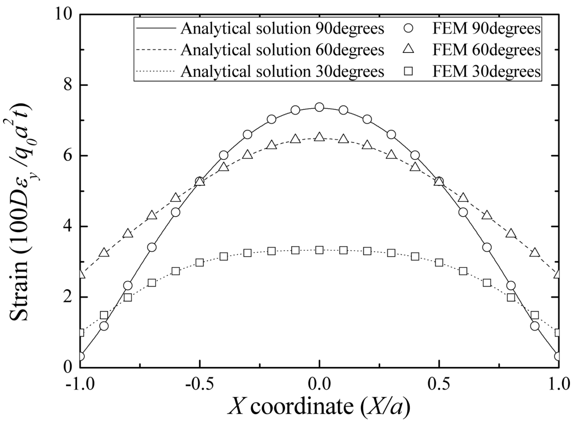

Fig. 6 Analytical and FEM solutions of y-direction strain in simply supported (SS2) isotropic skewed thin plate under uniform loading

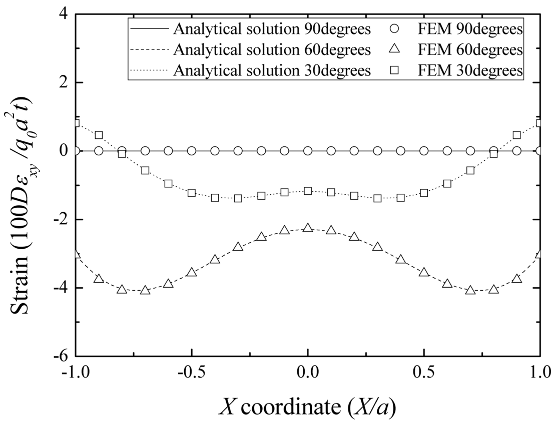

Fig. 7 Analytical and FEM solutions of shear strain of simply supported (SS2) isotropic skewed thin plate under uniform loading

with skew angle a, apparently due to reducing the shortest distance from the loading location to the nearest support. Strains ε_x and ε_y displayed in Figs. 5 and 6 also behave similarly for the same reason especially at the center of the plate. However, shear strain ε_{xy} in Fig. 7 is due to torsion and does not change with skew angle monotonically.

When a plate is skewed, the torsional effect becomes significant and it causes ε_{xy} in the plate. This relation is not monotonic, depending on the relative relations of the plate's skew angle, width/length ratio, loading position, boundary conditions, etc.

5.2 Simply supported isotropic skewed thick plates under a uniformly distributed load

In the previous example, it is proved that the present method can analyze thin plates with a large or small skewed angle very well. In this example, the skewed thick plates are analyzed. For the concerned skewed thick plates, the following geometrical properties are used: $a = b$, $t = 0.4\ a$. Like the previous example, uniformly distributed load q_0 is applied as an external force and $\alpha = 15°$, 30°, 45°, 60°, 75°, and 90° are employed as skewed angles. The SS2 boundary condition in Eq. (42) is used for all four edges. Fig. 8 is the deflection at the center of the plate of which skewed angle α = 30° of various m values against the number of terms l of a particular solution. Like the previous example (1), w of (l, m) = (5, 55) and (7, 35) differ less than 0.5% from that of (l, m)=(7, 55); therefore, (l, m)=(7, 55) is also employed in this example. Note that for different skew angles, similar results are observed.

For a comparison of the present analytical solution and other numerical solutions, Table 2 exhibits the results of the proposed solution, Liew and Han's research (1997), and an FEM analysis using ANSYS for the deflection w_c, maximum principal moment $M_{\max c}$, and minimum principal moment $M_{\min c}$ at the center of the plate (X, Y) = (0, 0). Figs. 9 to 12 display comparisons between the present method and FEM analysis using ANSYS for the deflection w and strains ε_x, ε_y, and ε_{xy} defined in Eq. (47) for α = 30°, 60°, and 90° along line HF defined in Fig. 1 and on the top of the plate. The deflection and strains are expressed in a dimensionless form as in the previous example. The results show that our analytical and the numerical solutions agree with each other very well for

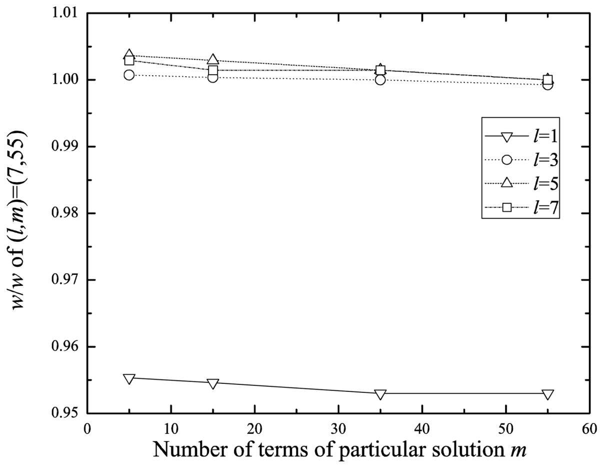

Fig. 8 Truncation effect for convergence for center deflection of simply supported (SS2) isotropic 30 degrees skewed thick plate under uniform loading

Table 2 Deflection, maximum moment, and minimum moment at the center of simply supported (SS2) skewed thick plates under uniform loading (value in parentheses is error ratio)

α		$100w_cD/q_0a^4$	$10M_{\max c}/q_0a^2$	$10M_{\min c}/q_0a^2$
	Present Study	8.0392	2.1469	1.9178
75°	ANSYS	8.0325 (-0.08%)	2.1431 (-0.18%)	1.9146 (-0.17%)
	Liew and Han (1997)	8.0236 (-0.19%)	2.1476 (0.03%)	1.9188 (0.05%)
	Present Study	5.8358	1.9177	1.5112
60°	ANSYS	5.8217 (-0.24%)	1.9067 (-0.57%)	1.5067 (-0.30%)
	Liew and Han (1997)	5.8319 (-0.07%)	1.9110 (-0.35%)	1.5108 (-0.03%)
	Present Study	3.1925	1.4581	0.9979
45°	ANSYS	3.1767 (-0.49%)	1.4509 (-0.49%)	0.9918 (-0.61%)
	Liew and Han (1997)	3.2095 (0.53%)	1.4548 (-0.23%)	0.9958 (-0.21%)
	Present Study	1.1383	0.8604	0.4889
30°	ANSYS	1.1342 (-0.36%)	0.8542 (-0.72%)	0.4848 (-0.84%)
	Liew and Han (1997)	1.1692 (2.71%)	0.8567 (-0.43%)	0.4885 (-0.08%)
	Present Study	0.1842	0.2784	0.1248
15°	ANSYS	0.1833 (-0.49%)	0.2768 (-0.57%)	0.1257 (0.72%)
	Liew and Han (1997)	0.1991 (8.09%)	0.2785 (0.04%)	0.1257 (0.72%)

these isotropic thick skewed plates under a uniformly distributed load.

A word of caution is in order here. It is shown from Figs. 4 and 9 that dimensionless deflection of skewed thick plate is more than that of skewed thin plate. This result is consistent with the fact described in chapter 1 that the Kirchhoff theory suffers from under-predicting deflections when thick plate is analyzed.

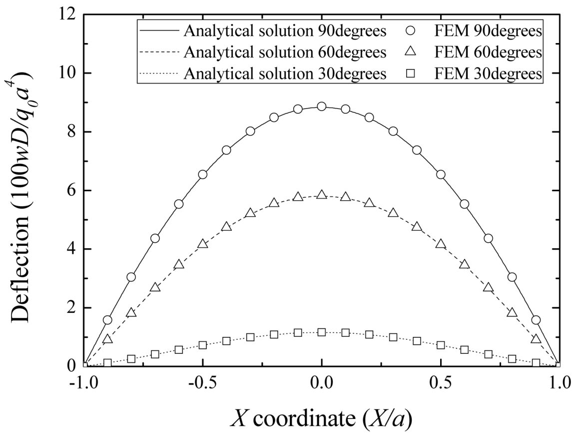

Fig. 9 Analytical and FEM solutions for deflection of simply supported (SS2) isotropic skewed thick plate under uniform loading

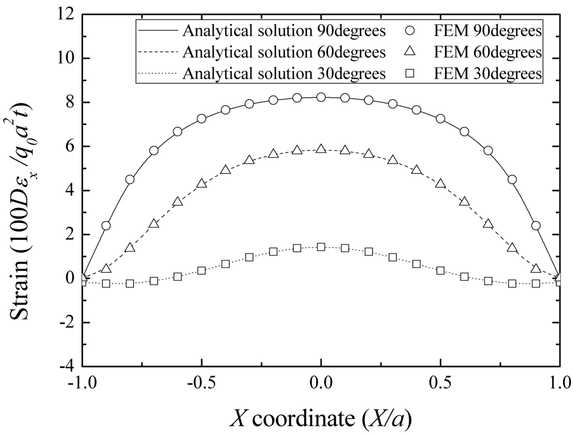

Fig. 10 Analytical and FEM results of x-direction strain of simply supported (SS2) isotropic skewed thick plate under uniform loading

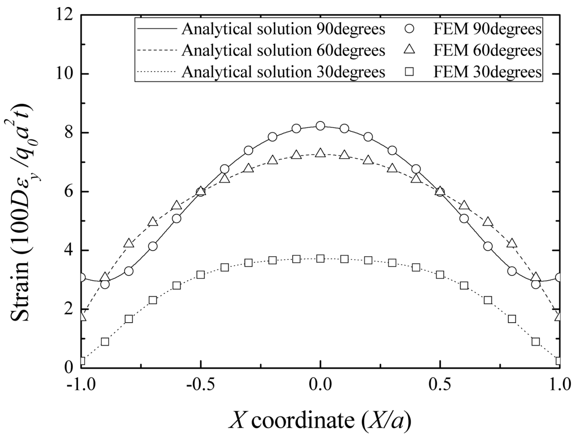

Fig. 11 Analytical and FEM solutions of y-direction strain in simply supported (SS2) isotropic skewed thick plate under uniform loading

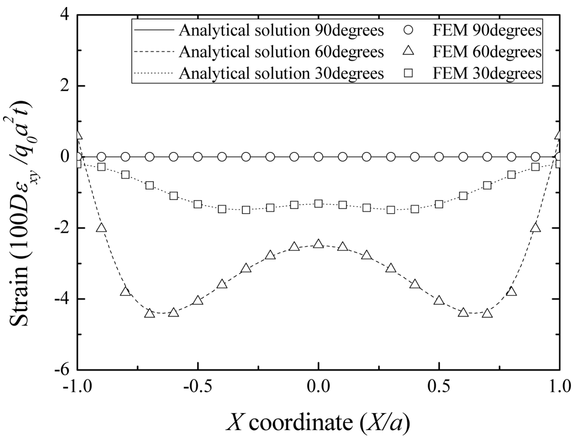

Fig. 12 Analytical and FEM solutions of shear strain of simply supported (SS2) isotropic skewed thick plate under uniform loading

5.3 Orthotropic thick skewed plates with two free edges and two clamped edges under a concentrated load

Orthotropic skewed thick plates are analyzed in this example, with the following material and geometrical properties: $E_y = 0.5\ E_x$, $G_{xy} = 0.3\ E_x$, $G_{xz} = 0.1\ E_x$, $G_{yz} = 0.08\ E_x$, $\nu_{xy} = 0.2$, $a = b$, $t = 0.4\ a$, where E_x and E_y are Young's modulus along the x and y directions, and G_{xy}, G_{xz}, and G_{yz} are shear modulus in the xy, xz, and yz planes. These values determine $[D_r]$, $[D_o]$, $[A_r]$, and $[A_o]$ in Eqs. (2) and (4). The external transverse force is a concentrated force of Q_0 applied at $(X, Y) = (-a/2, b/2)$. Plates with skew angle $\alpha = 30°$, $60°$, and $90°$ are analyzed here. Edges AB and CD are free and Edges BC and DA are clamped.

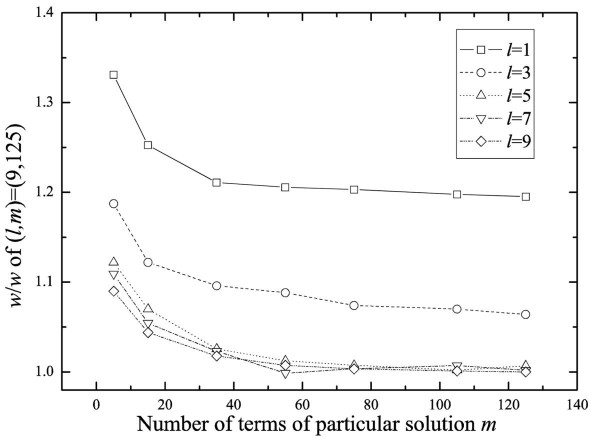

Fig. 13 Convergence of center deflection of orthotropic 30 degrees skewed thick plate under concentrated load

Table 3 Deflection, maximum moment, and minimum moment at the center of orthotropic skewed thick plates under concentrated loading (value in parentheses is error ratio)

α		$100w_cD_{11}/Q_0a^2$	$100w_lD_{11}/Q_0a^2$	$10M_{\max c}/Q_0$	$10M_{\min c}/Q_0$
60°	Present Study	3.7373	16.178	0.6351	-0.0096
	ANSYS	3.7719 (0.93%)	16.652(+2.93%)	0.6320 (-0.49%)	-0.0099 (3.12%)
30°	Present Study	3.8319	12.714	0.8740	0.0858
	ANSYS	3.7519 (-2.08%)	12.997(+2.18%)	0.8715 (-0.29%)	0.0841 (-1.98%)

As with the previous example, the numbers of terms including l and m need to be determined first. Fig. 13 shows the deflection w at the center of the plate $(X, Y) = (0, 0)$ for skew angle $\alpha = 30°$, as one of the cases considered, for various l and m values. It is seen that the deflection at $(l, m) = (9, 125)$ is well converged. Therefore $(l, m) = (9, 125)$ is employed here and is also used as the reference for comparison.

For this example, because no previous work in the literature has been found reporting a similar experience, only FEM analysis results by ANSYS are employed for comparison with our analytical solution results. Table 3 shows comparison results. In addition to w_c, $M_{\max c}$, and $M_{\min c}$ compared in the last two examples, the deflection at the loading point w_l is also compared. The deflection and moment are expressed in a dimensionless form as $100w_cD_{11}/Q_0a^2$ and $10M/Q_0$, where w and M are the deflection and moment, and D_{11} is the bending stiffness and is expressed as $D_{11} = E_xt^3/12(1-\nu_{xy}\nu_{yx})$.

Mindlin theory has drawback that the derivation of deflection is not continuous and it leads the deflection at the point where concentrated load generally expressed as a delta function is applied can be infinite. However, this research has expressed the concentrated load as the limited number of terms of trigonometric series, therefore the issue is automatically solved because it is no longer the delta function though it is very close to it. This prevents the deflection from being infinite, and it is seen from Table 3 that our solution is close enough to FEM result.

Figs. 14 to 17 show a comparison of the deflection w and strains ε_x, ε_y, and ε_{xy} defined in Eq. (28)

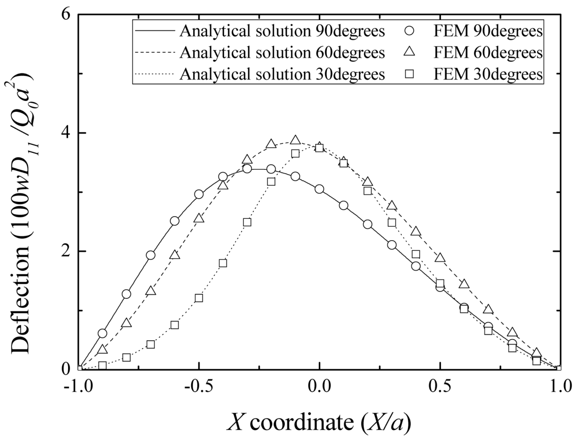

Fig. 14 Analytical and FEM solutions of center deflection of orthotropic skewed thick plate under concentrated load

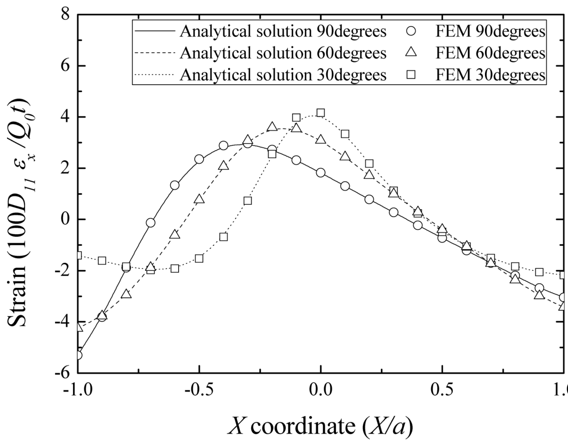

Fig. 15 Analytical and FEM solutions of x-direction strain of orthotropic skewed thick plate under concentrated load

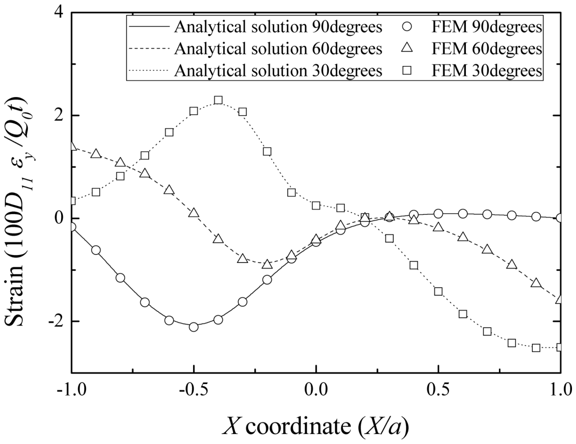

Fig. 16 Analytical and FEM solutions of y-direction strain of orthotropic skewed thick plate under concentrated load

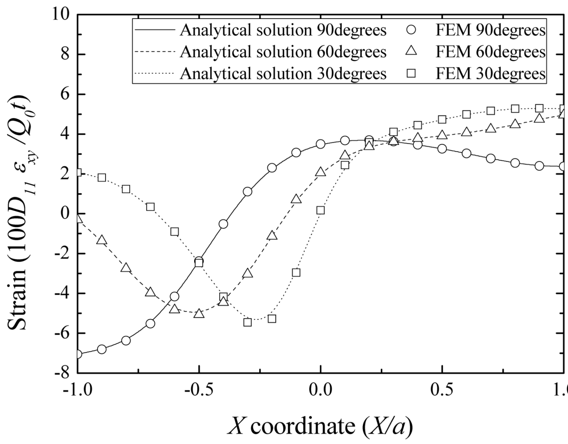

Fig. 17 Analytical and FEM solutions of shear strain of orthotropic skewed thick plate under concentrated load

for $\alpha = 30°$, 60°, and 90° along the line HF indicated in Fig. 1. The strains are normalized as $100D_{11}\varepsilon/Q_0t$. It is seen that our analytical solutions and the numerical solutions agree with each other very well.

The results shown in Figs. 14 to 17 indicate that the response behavior for this case is much more complex than the examples above, due to non-symmetric loading and boundary conditions. These response quantities are read at $Y = 0$. Due to the oblique coordinate system, the load at $(X, Y) = (-a/2, b/2)$ has different relative relations with the interested responses on $Y = 0$, along with different skew angles. For example, this causes the peak responses of the deflection in Fig. 14 moves towards center with the skew angle decreasing from 90° to 30° because the loading point of 30° plate is closer than that of 60° and 90° plate.

6. Conclusions

The governing differential equation of skewed thick plates in an oblique coordinate system is formulated in this paper. This equation allows derivation of the analytical solution for any boundary conditions and loading conditions. This derivation is reported for the first time. All response quantities, including shear forces, moments, stresses, strains, deflections, and rotation angles, can be readily derived from the proposed potential function ψ. The three illustrative examples show that the analytical solutions are in good agreement with those reported in several previous studies and with numerical solutions obtained by FEM. At the same time, it is found that some of the numerical results are not consistent with our exact solutions.

It is also worth noting that the approach to the governing differential equation and its analytical solution developed in this study can be used for further studies including, but not limited to, continuous plate analysis and dynamic analysis, for which only numerical solutions exist. For example, the solution presented here has been used to develop an analytical method for skewed composite beam bridge analysis, where the structure is considered to be composed of continuous thick plates. The details of this application will be reported in our next paper. Note that beam bridges represent the largest percentage of all bridge types in many countries and thus in the world. Meanwhile, as mentioned in the introduction, the solution developed here may provide the possibility of developing an analytical solution for a dynamic problem. For example, by introducing inertia terms to Eq. (29), the free vibration problem is expected to be solved.

Acknowledgements

The reported work was funded by the Michigan Department of Transportation, the US Federal Highway Administration, and Yonsei University Research Fund of 2010. This financial support is gratefully appreciated. However, the content of this paper reflects the views of the authors and not necessarily the sponsors.

References

Argyris, J.H. (1965), "Continua and discontinua", *Proceedings of Conference on Matrix Methods in Structural Mechanics*, Wright-Pat-terson Air Force Base, Ohio.

Butalia, T.S., Kant, T. and Dixit, V.D. (1990), "Performance of heterosis element for bending of skew rhombic plates", *Comput. Struct.*, **34**(1), 23-49.

Carstensen, C., Xie, X., Yu, G. and Zhou, T. (2010), "A priori and a posteriori analysis for a locking-free low order quadrilateral hybrid finite element for Reissner-Mindlin plates", *Comput. Meth. Appl. Mech. Eng.*, **200**(9-12), 1161-1175.

Cheung, Y.K. and Tham, L.G. (1998), *Finite Strip Method*, CRC Press, Boca Raton.

Civalek, Ö. (2009), "A four-node discrete singular convolution for geometric transformation and its application to numerical solution of vibration problem of arbitrary straight-sided quadrilateral plates", *Appl. Math. Model.*, **33**(1), 300-314.

Dawe, D.J. (1966), "Parallelogrammic elements in the solution of rhombic cantilever plate problems", *J. Strain Anal. Eng. Des.*, **1**(3), 223-230.

De Veubeke, B.F. and Sander, G. (1967), "An equilibrium model for plate bending", *Int. J. Solids Struct.*, **4**(4), 447-468.

Gangarao, H.V.S. and Chaudhary, V.K. (1998), “Analysis of skew and triangular plates in bending”, *Comput. Struct.*, **28**(2), 223-235.
Garcea, G., Madeo, A., Zagari, G. and Casciaro, R. (2009), “Asymptotic post-buckling FEM analysis using corotational formulation”, *Int. J. Solids Struct.*, **46**(2), 377-397.
Gürses, M., Civalek, Ö., Korkmaz, A.K. and Ersoy, H. (2009), “Free vibration analysis of symmetric laminated skew plates by discrete singular convolution technique based on first-order shear deformation theory”, *Int. J. Numer. Meth. Eng.*, **79**(3), 290-313.
Hangai, Y. (1995), *Fundamental Theory of Plates*, Shokokusha, Tokyo. (in Japanese)
Hencky, H. (1947), “Dber die Berficksichtigung der Schubverzerrungen in ebenen Platten”, *Ingenieur-Archiv*, **16**, 72- 76
Jirousek, J. (1987), “Hybrid-Trefftz plate bending elements with p-method capabilities”, *Int. J. Numer. Meth. Eng.*, **24**, 1367-1393.
Liao, H.W. and Huang, H.Y. (2008), “Buckling and postbuckling analyses of a skew plate”, *J. Mech.*, **24**(4), 347-355.
Liew, K.M. and Han, J.B. (1997), “Bending analysis of simply supported shear deformable skew plates”, *J. Eng. Mech.*, **123**(3), 214-221.
Liew, K.M., Huang, Y.Q. and Reddy, J.N. (2003), “Vibration analysis of symmetrically laminated plates based on FSDT using the moving least squares differential quadrature method”, *Comput. Meth. Appl. Mech. Eng.*, **192**(19), 2203-2222.
Liu, G.R., Nguyen-Thoi, T. and Lam, K.Y. (2008), “An edge-based smoothed finite element method (ES-FEM) for static and dynamic problems of solid mechanics”, *J. Sound Vib.*, **320**, 1100-1130.
Malekzadeh, P. and Karami, G. (2005), “Polynomial and harmonic differential quadrature methods for free vibration of variable thickness thick skew plates”, *Eng. Struct.*, **27**(10), 1563-1574.
Malekzadeh, P. (2008), “Differential quadrature large amplitude free vibration analysis of laminated skew plates based on FSDT”, *Compos. Struct.*, **83**(2), 189-200.
Mindlin, R.D. (1951), “Influence of rotatory inertia and shear on flexural motions of isotropic, elastic plates”, *J. Appl. Mech.*, **18**(1), 31-38.
Ming, P.G. and Song, L.F. (1987), “A new element used in the non-orthogonal boundary plate bending theory - an arbitrary quadrilateral element”, *Int. J. Numer. Meth. Eng.*, **24**, 1031-1042.
Mizusawa, T. and Kondo, Y. (2001), “Application of the spline element method to analyze vibration of skew Mindlin plates with varying thickness in one direction”, *J. Sound Vib.*, **241**(3), 485-501.
Mizusawa, T., Wada, H. and Nagino, H. (2007), “Free vibration analysis of skew Mindlin plates by the BF-spline Ritz method”, *JSCE J. Appl. Mech.*, **10**, 109-119. (in Japanese)
Monforton, G.R. and Schmit, L.A. (1968), “Finite element analysis of skew plates in bending (Skew parallelogram plates bending analyzed by finite element method, discussing stiffness and mass matrices application)”, *AIAA J.*, **6**, 1150-1152.
Morley, L.S.D. (1962), “Bending of a simply supported rhombic plate under uniform normal loading”, *The Quarterly Journal of Mechanics and Applied Mathematics*, **15**(4), 413-426.
Morley, L.S.D. (1963), *Skew Plates and Structures*, Pergamon Press, New York.
Muhammad, T. and Singh, A.V. (2004), “A p-type solution for the bending of rectangular, circular, elliptic and skew plates”, *Int. J. Solids Struct.*, **41**(15), 3977-3997.
Nguyen-Xuan, H., Rabczuk, T., Bordas, S. and Debongnie, J.F. (2008), “A smoothed finite element method for plate analysis”, *Comput. Meth. Appl. Mech. Eng.*, **197**(13-16), 1184-1203.
Nguyen-Xuan, H., Liu, G.R., Thai-Hoang, C. and Nguyen-Thoi, T. (2010), “An edge-based smoothed finite element method (ES-FEM) with stabilized discrete shear gap technique for analysis of Reissner-Mindlin plates”, *Comput. Meth. Appl. Mech. Eng.*, **199**(9-12), 471-489.
Ramadoss, P. and Nagamani, K. (2009), “Behavior of high-strength fiber reinforced concrete plates under in-plane and transverse loads”, *Struct. Eng. Mech.*, **31**(4), 371-382.
Ramesh, S.S., Wang, C.M., Reddy, J.N. and Ang, K.K. (2008), “Computation of stress resultants in plate bending problems using higher-order triangular elements”, *Eng. Struct.*, **30**, 2687-2706.
Ramesh, S.S., Wang, C.M., Reddy, J.N. and Ang, K.K. (2009), “A higher-order plate element for accurate prediction of interlaminar stresses in laminated composite plates”, *Compos. Struct.*, **91**(3), 337-357.

Razaqpur, A.G., Nofal, M. and Vasilescu, A. (2003), "An improved quadrilateral finite element for analysis of thin plates", *Finite Elem. Analy. Des.*, **40**(1), 1-23.

Reddy, J.N. (2007), *Theory and Analysis of Elastic Plates and Shells*, CRC Press, Taylor & Francis.

Reissner, E. (1945), "The effect of transverse shear deformation on the bending of elastic plates", *J. Appl. Mech.*, **12**, A69-A77.

Sengupta, D. (1991), "Stress analysis of flat plates with shear using explicit stiffness matrix", *Int. J. Numer. Meth. Eng.*, **32**, 1389-1409.

Sengupta, D. (1995), "Performance study of a simple finite element in the analysis of skew rhombic plates", *Comput. Struct.*, **54**(6), 1173-1182.

Szilard, R. (2004), *Theories and Applications of Plate Analysis*, John Wiley & Sons, Inc., Hoboken, New Jersey.

Tham, L.G., Li, W.Y., Cheung, Y.K. and Chen, M.J. (1986), "Bending of skew plates by spline-finite-strip method", *Comput. Struct.*, **22**(1), 31-38.

Timoshenko, S.P. and Woinowsky-Krieger, S. (1959), *Theory of Plates and Shells (2nd edition)*, Engineering Societies Monographs, McGraw-Hill, New York.

Wang, G. and Hsu, C.T.T. (1994), "Static and dynamic analysis of arbitrary quadrilateral flexural plates by B3-spline functions", *Int. J. Solids Struct.*, **31**(5), 657-667.